Frontiers in Health Informatics
ISSN-Online: 2676-7104
www.healthinformaticsjournal.com
2025; Vol 14: Issue 2
Open Access

Autophagy-Mediated Neuroendocrine Reprogramming by Trehalose in H841 Cells: Insights from Differential Gene Expression in Small Cell Lung Cancer

Pranoti Dhondage[1], Yash Hon[2], Hridya Ramesh[3], *Manju Shahare[4], Nikita Kokare[5]

[1,2,3,*4, 5], Department of Life Sciences and Biotechnology, Chhatrapati Shivaji Maharaj University, Navi Mumbai, Maharashtra

Corresponding Author: *Manju Shahare[4] E-mail address: manju.shahare@gmail.com

Cite this paper as: Pranoti Dhondage, Yash Hon, Hridya Ramesh, *Manju Shahare, Nikita Kokare (2025) Autophagy-Mediated Neuroendocrine Reprogramming by Trehalose in H841 Cells: Insights from Differential Gene Expression in Small Cell Lung Cancer. *Frontiers in Health Informatics, 14* (2), 2586-2598

Introduction: Small Cell Lung Cancer (SCLC) is a highly aggressive neuroendocrine carcinoma known for its rapid progression, high relapse rate, and pronounced phenotypic plasticity. The ability of SCLC cells to transition between neuroendocrine (NE) and non-NE states contributes to therapy resistance and tumor heterogeneity. Autophagy, a cellular degradation and recycling process, may influence this plasticity. Trehalose, a naturally occurring mTOR-independent autophagy enhancer.

Objective: This study aims to identify differentially expressed genes (DEGs) between trehalose-treated and untreated H841 SCLC cells using RNA sequencing, and to perform functional annotation and gene ontology (GO) analysis of these DEGs to understand the biological impact of autophagy.

B This study used the H841 SCLC cell line to investigate transcriptional changes following trehalose-induced autophagy. Public RNA-seq data (BioProject PRJNA1198304, GEO GSE284267) comprising three replicates each of control and trehalose-treated samples were processed using the Galaxy Europe platform. Quality control was performed using FastQC and Fastp; alignment to the human genome (GRCh38) was conducted with RNA STAR, and gene quantification with HTSeq-count. Differential expression analysis was carried out using DESeq2, and functional annotation via Metascape, DAVID, KEGG, and Cytoscape.

Results: A total of 12,132 DEGs were identified, including 7,041 upregulated and 5,091 downregulated genes. Key upregulated genes included GABARAP and NFE2L3, associated with autophagy and stress adaptation. KEGG analysis revealed downregulation of cell cycle-related pathways (e.g., ESCO1), while GO analysis highlighted enrichment in RNA processing, chromatin organization, and translation initiation. PCA and heatmap analyses confirmed distinct clustering of treated versus control samples, supporting a strong transcriptional response to trehalose.

Conclusion: Trehalose-induced autophagy significantly alters the transcriptome of SCLC cells by downregulating proliferation-associated genes and upregulating differentiation pathways, suggesting its potential role in modulating neuroendocrine plasticity, stress adaptation, and therapeutic response in aggressive tumor phenotypes.

Key words: *SCLC, Autophagy, Trehalose, Neuroendocrine Plasticity, RNA-Seq, Differential Gene Expression*

INTRODUCTION

Lung cancer remains a leading cause of cancer-related mortality worldwide, with Small Cell Lung Cancer (SCLC) representing one of its most aggressive subtypes. Characterized by rapid proliferation, early metastasis, and a high rate of relapse despite initial responsiveness to chemotherapy and radiotherapy, SCLC continues to pose significant therapeutic challenges1. The median survival for patients with extensive-stage SCLC remains less than a year, underscoring the urgent need for novel therapeutic strategies and deeper molecular insights. Unlike Non-Small Cell Lung Cancer (NSCLC), SCLC displays a remarkable degree of lineage plasticity, particularly in its ability to transition between neuroendocrine (NE) and non-NE phenotypes2. This dynamic phenotypic reprogramming contributes substantially to treatment resistance, tumour heterogeneity, and disease progression.

SCLC is histologically defined by small, round, blue cells and is molecularly marked by the frequent loss of tumour suppressor genes such as TP53 and RB1. It commonly exhibits neuroendocrine differentiation, characterized by the expression of markers such as ASCL1, NEUROD1, CHGA, and SYP3,4. Recent studies have highlighted the plasticity of SCLC cells and their ability to shift between transcriptional states in response to microenvironmental cues or therapeutic stress. This neuroendocrine plasticity allows tumour cells to adapt, evade cytotoxic treatments, and adopt more invasive phenotypes, emphasizing the need to understand the underlying regulatory mechanisms5.

Emerging evidence suggests that autophagy a conserved catabolic process that enables cells to recycle cytoplasmic components under stress may influence neuroendocrine differentiation and plasticity6. Autophagy plays a dual role in cancer: it can suppress tumour initiation by maintaining cellular homeostasis, yet in established cancers, it often supports survival under metabolic or therapeutic stress5. While the role of autophagy in various cancers has been widely studied, its involvement in the phenotypic plasticity of SCLC remains poorly understood7. Understanding this connection could offer novel insights into tumour evolution, therapy resistance, and potential intervention strategies.

Trehalose, a naturally occurring disaccharide, has been recognized as an effective autophagy enhancer that operates independently of the mTOR pathway. It has been shown to promote autophagic flux and facilitate the clearance of misfolded proteins and damaged organelles, particularly in neurodegenerative models8,9. In contrast to conventional autophagy inducers like rapamycin, trehalose induces autophagy without inhibiting mTOR, making it a promising pharmacological tool with reduced toxicity. Although trehalose has been studied in various disease models, its role in modulating cancer cell phenotypes, particularly in the context of SCLC neuroendocrine plasticity, remains largely unexplored. The H841 cell line is a well-characterized human SCLC model that exhibits neuroendocrine features, making it suitable for exploring transcriptional changes associated with phenotypic transitions. By leveraging trehalose-induced autophagy in H841 cells, we aim to investigate whether autophagy activation leads to gene expression changes linked to neuroendocrine reprogramming10. This study employs high-throughput RNA sequencing (RNA-seq) to identify differentially expressed genes (DEGs) and to annotate the pathways influenced by trehalose treatment.

OBJECTIVES

The primary objective of this study is to investigate the transcriptional impact of autophagy induction in small cell lung cancer (SCLC) cells using a high-throughput RNA sequencing (RNA-seq) approach. Specifically, we aim to perform a comprehensive RNA-seq analysis of paired trehalose-treated (H841-Tre)

and untreated control (H841) cell lines to identify differentially expressed genes (DEGs) associated with trehalose-induced autophagy. By comparing the gene expression profiles between these two conditions, we seek to uncover key molecular alterations and regulatory pathways influenced by autophagy activation in the SCLC context. Furthermore, we aim to perform in-depth functional annotation and gene ontology (GO) enrichment analysis of the identified DEGs to interpret their biological significance. This includes categorizing the DEGs into relevant biological processes, cellular components, and molecular functions, as well as mapping them to enriched signaling pathways using established bioinformatics tools. Through this analysis, we intend to gain insights into how autophagy modulates gene expression networks and contributes to neuroendocrine plasticity, cellular stress response, and potential phenotypic shifts in SCLC cells.

METHODS

This study utilized the human small cell lung cancer (SCLC) cell line H841 to investigate transcriptional changes in response to autophagy induction. Trehalose, a disaccharide known to stimulate autophagy via mTOR-independent pathways, was administered to the treatment group, while untreated H841 cells served as the control. Specific treatment concentration and duration were followed as per the experimental design in the original dataset. Three biological replicates were included for each group, resulting in six total samples.

Data Acquisition - Publicly available RNA sequencing data were obtained from the NCBI Sequence Read Archive (SRA) under BioProject accession PRJNA1198304 and GEO Series GSE284267. FASTQ files corresponding to three control and three trehalose-treated H841 samples were downloaded using the "Faster Download and Extract Reads in FASTQ" tool within the Galaxy Europe platform (https://usegalaxy.eu/), ensuring consistent data handling from acquisition to analysis11.

The RNA-Seq data analysis followed a systematic, multi-step workflow designed to ensure high-quality processing and accurate interpretation of gene expression changes in trehalose-treated versus control H841 small cell lung cancer (SCLC) cells. In the initial quality control step, raw sequencing reads were evaluated using FastQC, which provided detailed metrics on per-base quality scores, GC content, adapter contamination, and sequence duplication levels. To facilitate comparative evaluation across all six samples, MultiQC was employed to aggregate the FastQC outputs into a single, comprehensive report. Following quality assessment, raw reads were subjected to adapter trimming and quality filtering using Fastp12. This step removed low-quality bases and residual adapter sequences, thereby improving the reliability of downstream alignments. The success of trimming was validated by re-running FastQC, which showed marked improvements in base quality scores and reduced presence of adapter contamination.

Next, the high-quality filtered reads were aligned to the Homo sapiens reference genome (GRCh38/hg38) using the RNA STAR aligner in two-pass mode. STAR was selected for its robustness in mapping spliced reads, which is particularly important in the context of eukaryotic transcriptome analysis13. The alignment process generated sorted BAM files, which formed the basis for quantification and downstream expression analysis. For gene-level quantification, aligned reads were processed using HTSeq-count in 'union' mode, referencing the GRCh38 gene annotation file in GTF format. Only reads that mapped uniquely to exonic regions were counted to ensure specificity. The resulting raw count matrix provided gene-wise expression values across all samples.

Differential gene expression analysis was performed using DESeq2, which models count data with a

negative binomial distribution. Internal normalization was applied using the median-of-ratios method to correct for differences in sequencing depth and library composition. Statistical testing was conducted to identify genes that were significantly differentially expressed between trehalose-treated and control groups, using a false discovery rate (FDR) threshold of adjusted p-value < 0.05 and an absolute $\log_2$ fold change ≥ 1. DESeq2's output was visualized using tools available in the Galaxy platform to generate PCA plots, heatmaps, volcano plots, and MA plots, providing insight into expression trends and sample clustering14.

To determine the biological significance of differentially expressed genes (DEGs), functional annotation and pathway enrichment analysis were conducted using Metascape, along with support from DAVID and UniProt databases15. These tools facilitated the identification of enriched Gene Ontology (GO) terms, KEGG pathways, and molecular functions associated with DEGs. The results were categorized into biological processes, molecular functions, and cellular components16,17. Finally, Cytoscape was used to visualize gene–pathway interaction networks, uncovering key regulatory modules and potential biological mechanisms affected by trehalose-induced autophagy in H841 cells18.

All analysis steps were documented within Galaxy's built-in history function, preserving tool parameters, intermediate files, and final outputs. This ensured full reproducibility and transparency of the computational workflow, allowing re-execution and validation of the analysis pipeline.

The analysis was performed entirely on the Galaxy Europe platform, ensuring transparency, reproducibility, and accessibility throughout the workflow19. Beginning with raw data acquisition from NCBI's SRA database, we conducted rigorous quality control, read alignment, and quantification steps using established tools such as FastQC, RNA STAR, HTSeq-count, and DESeq2. Functional annotation and biological interpretation were carried out using DAVID, UniProt, and KEGG, supplemented by network visualization through Cytoscape. In the next chapter, we will present the results derived from this pipeline, including key differentially expressed genes, enriched biological processes, and the interpretation of how trehalose-induced autophagy20,21 may influence cellular phenotype in the context of SCLC.

RESULTS

Overview of RNA-Seq Analysis

To investigate transcriptional alterations associated with trehalose-induced autophagy in small cell lung cancer (SCLC), RNA-sequencing was performed on H841 cells treated with trehalose (H841-Tre) and untreated controls. Six samples (three biological replicates per condition) were retrieved from NCBI SRA under BioProject ID PRJNA1198304 and processed through a standardized RNA-Seq pipeline. This included quality control, trimming, alignment to the human genome (GRCh38/hg38), quantification, and differential expression analysis using DESeq2. Functional annotation was performed using Metascape, Gene Ontology (GO), and KEGG enrichment tools.

Quality Control and Preprocessing

Initial quality assessment of raw reads using FastQC revealed high sequencing quality (Phred score >30) across all samples, with minimal adapter contamination.

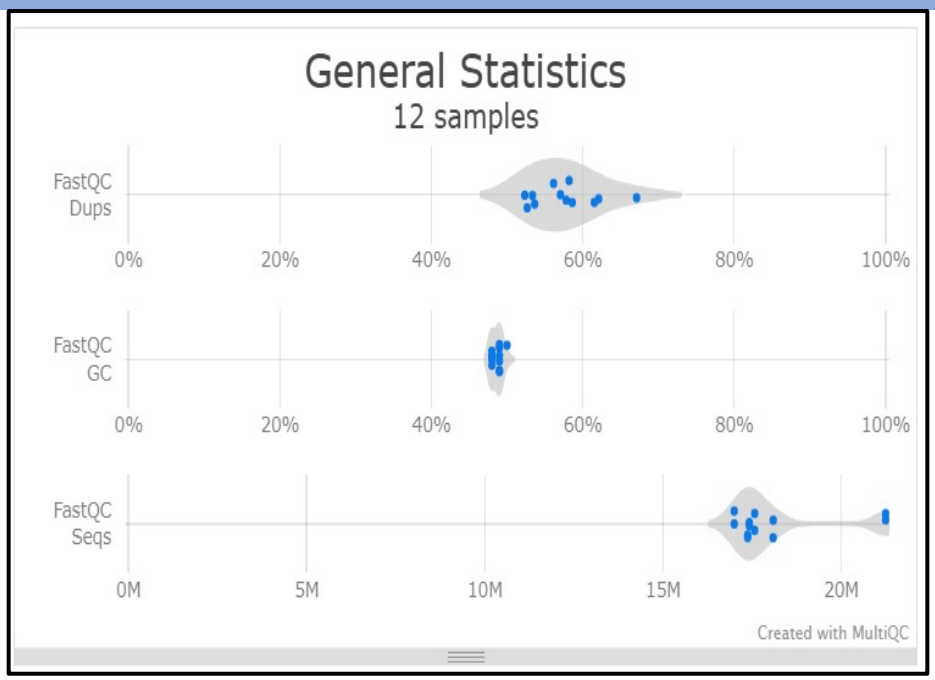

Fig. 1. General Statistics

The average GC content ranged from 48–50%, and duplication levels varied between 51.8% and 66.0%. Adapter trimming and filtering were performed using Fastp. Post-trimming FastQC results confirmed improved read quality, rendering the data suitable for downstream analysis (Table 1).

Table 1. FastQC metrics for raw RNA-Seq reads.

Sr. No.	Sample Name	Dups	GC	Seqs
1	SRR31716603_1	55.9%	48.0%	17.6M
2	SRR31716603_2	51.8%	49.0%	17.6M
3	SRR31716604_1	57.0%	48.0%	17.2M
4	SRR31716604_2	52.8%	49.0%	17.2M
5	SRR31716605_1	66.0%	49.0%	21.5M
6	SRR31716605_2	61.5%	50.0%	21.5M
7	SRR31716606_1	60.3%	48.0%	18.3M
8	SRR31716606_2	55.5%	49.0%	18.3M
9	SRR31716607_1	57.4%	48.0%	17.6M
10	SRR31716607_2	53.1%	49.0%	17.6M
11	SRR31716608_1	56.6%	48.0%	17.8M
12	SRR31716608_2	52.1%	49.0%	17.8M

Alignment and Quantification

Trimmed reads were aligned to the GRCh38 reference genome using RNASTAR. All samples achieved >95% total alignment rate with an average unique mapping rate of ~85%, confirming high data integrity.

Gene-level quantification was performed using HTSeq-count, resulting in a raw count matrix covering ~19,500 genes across all samples.

Differential Gene Expression Analysis

Differential gene expression analysis using DESeq2 identified 12,132 significant DEGs between trehalose-treated and control cells. Of these, 7,041 genes were upregulated and 5,091 were downregulated (adjusted $p < 0.05$). Dimensionality reduction using principal component analysis (PCA) demonstrated clear separation between treatment groups, while heatmaps and dispersion plots indicated good replicate consistency and appropriate model fit (Figures 2–6).

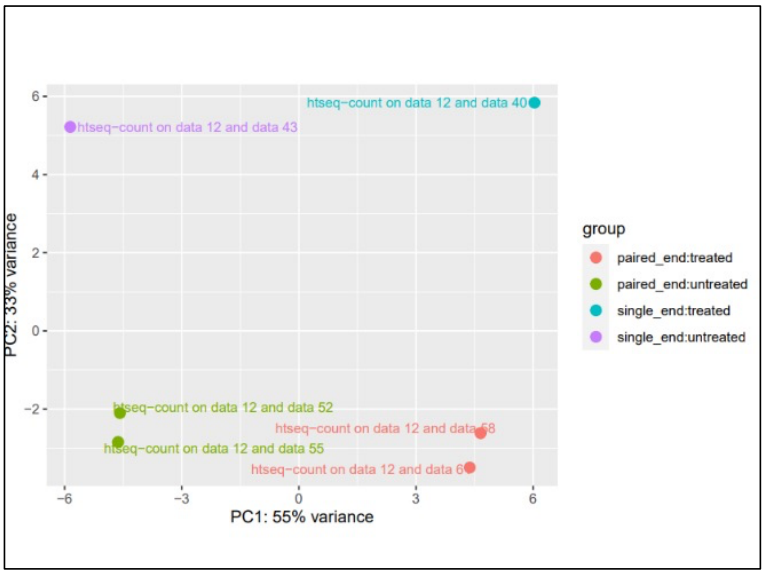

Fig. 2. PCA plot showing sample clustering

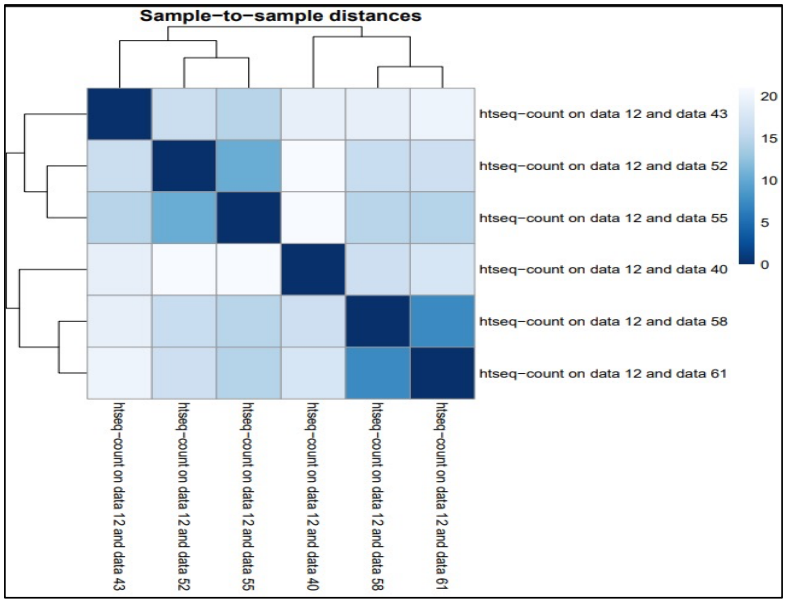

Fig. 3. Heatmap

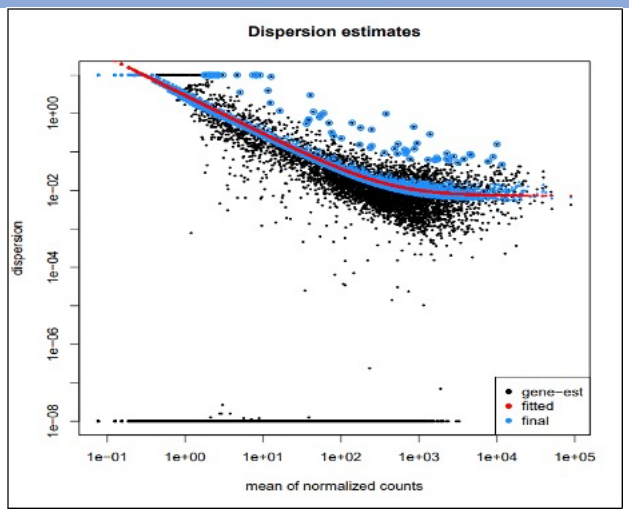

Fig. 4. Dispersion estimate plot

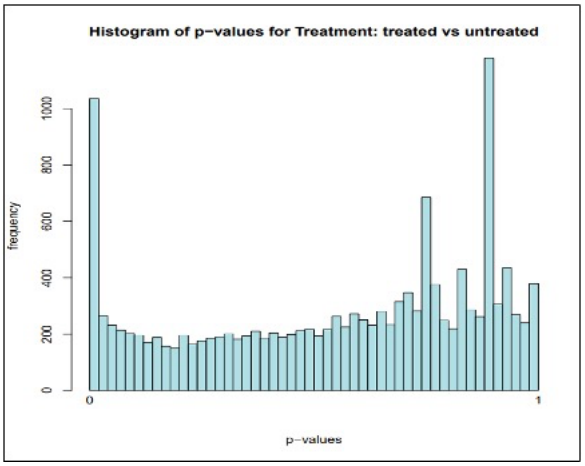

` Fig. 5. P-value histogram.

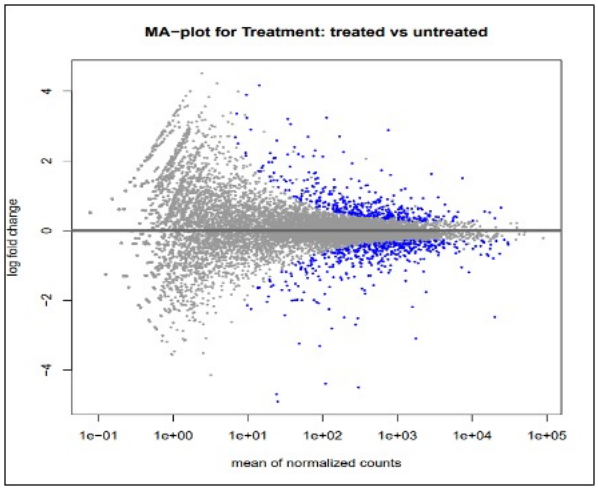

Fig. 6. MA-plot

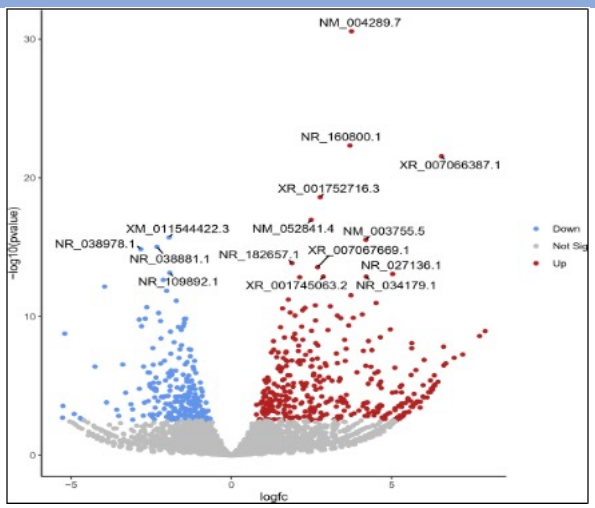

Fig. 7. Volcano plot

Principal Component Analysis (PCA) revealed a clear separation between trehalose-treated and control H841 samples, indicating a strong treatment-induced effect on global gene expression that outweighed any batch or technical variation. The accompanying heatmap demonstrated sample-to-sample similarities, with darker blue diagonals confirming high intra-group consistency and effective clustering between biological replicates. The dispersion plot showed a characteristic trend of decreasing dispersion with increasing mean expression, validating the reliability of dispersion estimates used in the DESeq2 model. A histogram of p-values displayed a strong enrichment of low p-values, further supporting the presence of numerous significantly differentially expressed genes (DEGs) and suggesting real biological differences between the two groups rather than random variation. The MA plot visualized $\log_2$ fold changes versus mean expression, clearly distinguishing upregulated and downregulated genes from those with no significant change, while the volcano plot provided a comprehensive overview of DEGs by plotting $\log_2$ fold change against the negative $\log_{10}$ adjusted p-value. In the volcano plot, red dots represented significantly upregulated genes, blue dots denoted downregulated genes, and grey dots indicated genes with no significant expression change. Together, these visualizations provide a robust representation of the transcriptional landscape altered by trehalose treatment, highlighting key genes and pathways affected by autophagy induction in SCLC cells.

Table 2. Selected top DEGs with biological function annotations.

Gene Symbol	$\log_2$(FC)	P-value	Function
NFE2L3	3.75	2.70×10^{-31}	Transcription factor involved in stress response
MIR1915HG	3.70	4.64×10^{-23}	lncRNA host gene
GABARAP	4.34	2.76×10^{-22}	Regulator of autophagy and intracellular trafficking
DEPP1	−0.002	0.999	Autophagy regulator, non-significant

KEGG Pathway Enrichment: Cell Cycle Modulation

KEGG pathway analysis revealed enrichment of DEGs in pathways associated with signal transduction and cell cycle regulation. The "Cell Cycle" pathway (hsa04110) was notably downregulated. ESCO1, essential for sister chromatid cohesion, was significantly repressed, suggesting impaired mitotic progression in trehalose-treated cells (Figure 7). These findings align with transcriptomic trends observed in the GO analysis, which pointed to downregulation of cell proliferation pathways and upregulation of autophagy-related processes. Together, these data suggest that trehalose-induced autophagy may suppress cell cycle progression, potentially diverting energy toward cellular stress responses and promoting a more differentiated or quiescent state in SCLC cells.

Functional Annotation and Pathway Analysis

Gene annotation using Metascape revealed enrichment of upregulated genes involved in nuclear transport, RNA processing, and vesicle-mediated transport. Notably, DGCR5 and NUP43 were among the most upregulated genes. Downregulated genes included those associated with cell cycle and DNA replication.

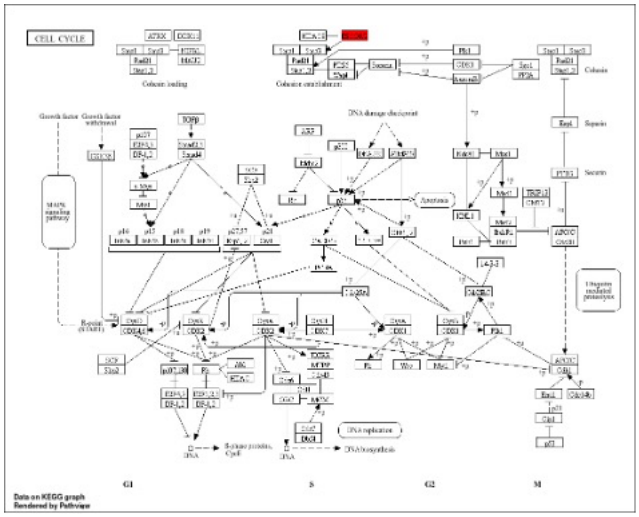

Fig 8. KEGG Pathway

Gene Ontology (GO) Enrichment Analysis

To explore the functional implications of differentially expressed genes (DEGs) between trehalose-treated and control H841 small cell lung cancer (SCLC) cells, GO enrichment analysis was performed across three main categories: Biological Process (BP), Cellular Component (CC), and Molecular Function (MF).

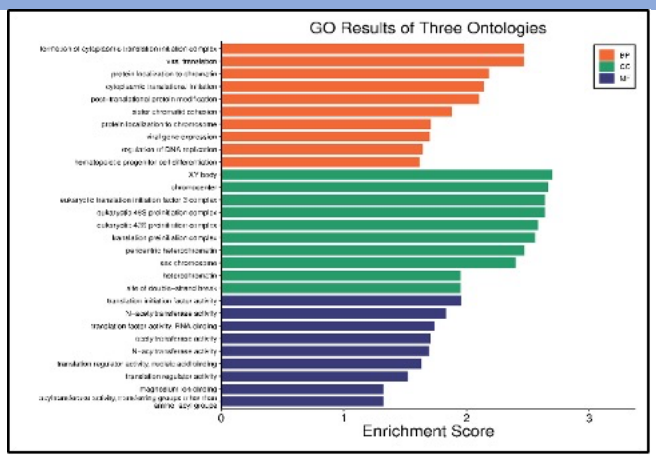

Fig 9. Gene Ontology Enrichment Analysis of top 15 genes

BP: Enriched in RNA processing, chromatin organization, cytoplasmic translation initiation.
CC: Enriched in chromocenters, translation initiation complexes, and heterochromatin structures.
MF: Enriched in RNA-binding, acetyl transferase activity, translation initiation factor activity.

In this study, transcriptomic profiling of trehalose-treated H841 small cell lung cancer (SCLC) cells revealed substantial gene expression alterations associated with autophagy induction. A total of 12,132 differentially expressed genes (DEGs) were identified, including 7,041 upregulated and 5,091 downregulated genes. Gene Ontology (GO) analysis showed strong enrichment in processes such as cytoplasmic translation initiation, chromatin organization, and protein modification, indicating activation of stress adaptation and regulatory pathways. Cellular component analysis highlighted changes in nuclear structures like chromocenters and heterochromatin, while molecular function analysis revealed enrichment of RNA-binding proteins, acetyltransferases, and translation regulators. KEGG pathway mapping of the cell cycle revealed downregulation of critical genes like ESCO1, involved in cohesion establishment, suggesting suppression of proliferation-related pathways. Together, these results demonstrate that trehalose-induced autophagy drives a broad transcriptional shift away from cell cycle progression and toward differentiation, stress response, and neuroendocrine plasticity, supporting the hypothesis that autophagy plays a regulatory role in tumor phenotype adaptation in SCLC.

DISCUSSION

This study provides transcriptomic evidence that pharmacological induction of autophagy by trehalose leads to significant gene expression changes in H841 small cell lung cancer (SCLC) cells. RNA-seq analysis identified 12,132 differentially expressed genes (DEGs), including upregulation of autophagy-related genes and downregulation of key proliferative and cell cycle regulators. Functional enrichment analyses revealed activation of pathways associated with autophagy, calcium signaling, axon guidance, and neurotrophin signaling, alongside suppression of DNA replication and p53 signaling pathways. Importantly, the data suggest that autophagy influences neuroendocrine plasticity in SCLC by modulating transcriptional programs linked to cell identity and stress adaptation22. The observed enrichment of neuronal differentiation and developmental signaling pathways, coupled with reduced expression of proliferation-related genes, supports a model in which autophagy facilitates a shift from a proliferative to a more differentiated or adaptive cellular phenotype23. Furthermore, several long non-coding RNAs and nuclear transport genes were differentially expressed, indicating broader regulatory roles for autophagy in

transcriptome remodelling24. Collectively, these findings suggest that autophagy, beyond its traditional role in cellular recycling, may act as a regulatory mechanism in lineage plasticity, contributing to tumor heterogeneity and therapy resistance in SCLC. Trehalose, by modulating autophagic pathways, emerges as a promising tool for dissecting the molecular basis of neuroendocrine reprogramming and may hold potential as an adjunct therapeutic strategy in managing aggressive and plastic tumor states25.

CONCLUSSION

This study provides comprehensive transcriptomic evidence that pharmacological activation of autophagy via trehalose induces substantial gene expression alterations in H841 small cell lung cancer (SCLC) cells. Through high-throughput RNA sequencing and rigorous bioinformatic analysis, we identified 12,132 differentially expressed genes, including significant upregulation of autophagy-related genes and concurrent downregulation of key regulators of cell proliferation and the cell cycle. Functional annotation and pathway enrichment analyses revealed that trehalose treatment activates cellular processes related to RNA processing, chromatin organization, and stress adaptation, while suppressing mitotic progression and DNA replication pathways. These findings support the hypothesis that autophagy plays a regulatory role in modulating neuroendocrine plasticity in SCLC, potentially contributing to phenotype switching, tumor heterogeneity, and therapy resistance. The use of trehalose, a non-toxic, mTOR-independent autophagy enhancer, offers a promising approach to investigating autophagy-mediated transcriptional reprogramming and may serve as a potential adjunct in therapeutic strategies aimed at targeting lineage plasticity in aggressive SCLC subtypes. Future studies involving in vivo validation and functional assays are warranted to translate these transcriptomic insights into clinical applications.

ACKNOWLDGEMENT

We would like to express our deepest gratitude to RASA Life Science Informatics, Pune, Maharashtra for their support through out the completion of this work.

CONFLICT OF INTEREST

None

REFRENCES

[1] Gazdar, Adi F., Paul A. Bunn, and John D. Minna. "Small-cell lung cancer: what we know, what we need to know and the path forward." Nature Reviews Cancer 17, no. 12 (2017): 725-737.

[2] Boumahdi, Soufiane, and Frederic J. de Sauvage. "The great escape: tumour cell plasticity in resistance to targeted therapy." Nature reviews Drug discovery 19, no. 1 (2020): 39-56.

[3] George, Julie, Jing Shan Lim, Se Jin Jang, Yupeng Cun, Luka Ozretić, Gu Kong, Frauke Leenders et al. "Comprehensive genomic profiles of small cell lung cancer." Nature 524, no. 7563 (2015): 47-53.

[4] Vitale, Elsa, Alessandro Rizzo, Lorenza Maistrello, Deniz Can Guven, Omar Cauli, Domenico Galetta, and Vito Longo. "Treatment-Related Adverse Events in Extended Stage Small Cell Lung Cancer Patients Receiving First-Line Chemoimmunotherapy Versus Chemotherapy Alone: A Systematic Review and Meta-Analysis." Cancers 17, no. 9 (2025): 1571.

[5] Ireland, Abbie S., Sarah B. Hawgood, Daniel A. Xie, Margaret W. Barbier, Scarlett Lucas-Randolph, Darren R. Tyson, Lisa Y. Zuo et al. "Basal cell of origin resolves neuroendocrine-tuft lineage plasticity in cancer." bioRxiv (2024): 2024-11.

[6] Simpson, Kathryn L., Dominic G. Rothwell, Fiona Blackhall, and Caroline Dive. "Challenges of

small cell lung cancer heterogeneity and phenotypic plasticity." Nature Reviews Cancer (2025): 1-16.
[7] Yin, Evan, Motoyasu Satou, and Toru Tateno. "Targeting Autophagy for Pituitary Tumors." Cancers 17, no. 9 (2025): 1402.
[8] Yang, Jingchao, Longhui Yuan, Lan Li, Fei Liu, Jingping Liu, Younan Chen, Ping Fu, Yanrong Lu, and Yujia Yuan. "Trehalose activates autophagy to alleviate cisplatin-induced chronic kidney injury by targeting the mTOR-dependent TFEB signaling pathway." Theranostics 15, no. 6 (2025): 2544.
[9] Zheng, Chun-Yan, Sze-Kwan Lam, Yuan-Yuan Li, and James Chung-Man Ho. "Arsenic trioxide-induced cytotoxicity in small cell lung cancer via altered redox homeostasis and mitochondrial integrity." International journal of oncology 46, no. 3 (2015): 1067-1078.
[10] Dobin, Alexander, Carrie A. Davis, Felix Schlesinger, Jorg Drenkow, Chris Zaleski, Sonali Jha, Philippe Batut, Mark Chaisson, and Thomas R. Gingeras. "STAR: ultrafast universal RNA-seq aligner." Bioinformatics 29, no. 1 (2013): 15-21.
[11] “The Galaxy platform for accessible, reproducible, and collaborative data analyses: 2024 update." Nucleic acids research 52, no. W1 (2024): W83-W94.
[12] Shannon, Paul, Andrew Markiel, Owen Ozier, Nitin S. Baliga, Jonathan T. Wang, Daniel Ramage, Nada Amin, Benno Schwikowski, and Trey Ideker. "Cytoscape: a software environment for integrated models of biomolecular interaction networks." Genome research 13, no. 11 (2003): 2498-2504.
[13] Zhang, Jing, Xiaoping Zeng, Qiji Guo, Zhenxin Sheng, Yan Chen, Shiyue Wan, Lele Zhang, and Peng Zhang. "Small cell lung cancer: emerging subtypes, signaling pathways, and therapeutic vulnerabilities." Experimental Hematology & Oncology 13, no. 1 (2024): 78.
[14] Love, Michael I., Wolfgang Huber, and Simon Anders. "Moderated estimation of fold change and dispersion for RNA-seq data with DESeq2." Genome biology 15 (2014): 1-21.
[15] Huang, Da Wei, Brad T. Sherman, and Richard A. Lempicki. "Systematic and integrative analysis of large gene lists using DAVID bioinformatics resources." Nature protocols 4, no. 1 (2009): 44-57.
[16] Kanehisa, Minoru, Miho Furumichi, Yoko Sato, Mari Ishiguro-Watanabe, and Mao Tanabe. "KEGG: integrating viruses and cellular organisms." Nucleic acids research 49, no. D1 (20gttg21): D545-D551.
[17] Zhang, Yongxiang, Feng Chen, Yuqi Cao, Hao Zhang, Lingling Zhao, and Yijun Xu. "Identifying diagnostic markers and establishing prognostic model for lung cancer based on lung cancer-derived exosomal genes." Cancer Biomarkers 42, no. 2 (2025): 18758592251317400.
[18] Hao, Yujie, Mingchen Li, Wenxu Liu, Zhenyi Ma, and Zhe Liu. "Autophagic flux modulates tumor heterogeneity and lineage plasticity in SCLC." Frontiers in Oncology 14 (2025): 1509183.
[19] Radbakhsh, Shabnam, Diana Marisol Abrego-Guandique, Tiziana Bacchetti, Seyed Hamid Aghaee-Bakhtiari, Ali Mahmoudi, Ali Akhonpour Manteghi, Mohammad Javad Bazyari, Erika Cione, Gianna Ferretti, and Amirhossein Sahebkar. "Direct hybridization and bioinformatics analysis of circulating microRNAs in patients with Alzheimer’s disease under intravenous trehalose treatment." Brain Research 1857 (2025): 149607.
[20] Joshi, Asim, Nivitha Bhaskar, and Joel D. Pearson. "Neuroendocrine Transformation as a Mechanism of Resistance to Targeted Lung Cancer Therapies: Emerging Mechanisms and Their Therapeutic Implications." Cancers 17, no. 2 (2025): 260.
[21] Statello, Luisa, Chun-Jie Guo, Ling-Ling Chen, and Maite Huarte. "Gene regulation by long non-

coding RNAs and its biological functions." Nature reviews Molecular cell biology 22, no. 2 (2021): 96-118.
[22] Oser, Matthew G., Matthew J. Niederst, Lecia V. Sequist, and Jeffrey A. Engelman. "Transformation from non-small-cell lung cancer to small-cell lung cancer: molecular drivers and cells of origin." The Lancet Oncology 16, no. 4 (2015): e165-e172.
[23] Desai, Parth, and Anish Thomas. "Small Cell Lung Cancer: New Hope, New Challenges." JCO Oncology Advances 1 (2024): e2400019.
[24] Mizushima, Noboru, and Masaaki Komatsu. "Autophagy: renovation of cells and tissues." Cell 147, no. 4 (2011): 728-741.
[25] Kim, Sunghwan, Jie Chen, Tiejun Cheng, Asta Gindulyte, Jia He, Siqian He, Qingliang Li et al. "PubChem in 2021: new data content and improved web interfaces." Nucleic acids research 49, no. D1 (2021): D1388-D1395.